Fabrication and properties of the meander nanowires based on ultra-thin Nb films*

Zhao Lu(赵 璐), Jin Yi-Rong(金贻荣), Li Jie(李 洁),
Deng Hui(邓 辉), and Zheng Dong-Ning(郑东宁)†

Beijing National Laboratory for Condensed Matter Physics, Institute of Physics, Chinese Academy of Sciences, Beijing 100190, *China*

(Received 7 April 2014; revised manuscript received 23 April 2014; published online 10 June 2014)

We report the fabrication and the study of superconducting properties of ultra-thin Nb superconducting meander nanowires, which can be used as superconducting nanowire single-photon detectors (SNSPDs). The ultra-thin (about 7-nm thick) Nb films are patterned into micro-bridges, and 100-nm wide meander nanowires by using e-beam lithography (EBL). The average transition temperature (T_c) of the nanowires is about 4.8 K and the critical current density j_c is about 2.8×10^6 A/cm^2. Superconducting characteristics of the specimens at different applied magnetic fields up to 8 T (parallel or perpendicular to the specimen) are systematically investigated. The normalized temperature t ($=T/T_c$) dependences of the parallel critical field ($H_{c\parallel}$) for both the micro-bridge and the meander nanowire are almost the same, following the Ginzburg and Landau (GL) formalism for ultra-thin films. However, in perpendicular field and in the vicinity of T_c ($>0.95T_c$), the critical field $H_{c\perp}$ of the nanowire exhibits a down-turn curvature nonlinear temperature dependence while the micro-bridge displays a linear temperature dependence. The nonlinear behavior of $H_{c\perp}$ in the nanowire is believed to be due to the fact that in the vicinity of T_c the coherence length becomes larger than the line width. Additionally, the localization of carriers in the nanowire could also contribute to the nonlinear behavior. The resistive transitions could be described by the phase-slip model for quasi-one-dimensional system. Moreover, the hysteresis in I–V curve of the meander nanowires can be illustrated by a simple model of localized normal hotspot maintained by Joule heating.

Keywords: Nb meander nanowire, critical temperature, critical field, critical current

PACS: 74.78.–w, 74.25.F–, 81.16.Rf, 81.07.Gf **DOI:** 10.1088/1674-1056/23/8/087402

1. Introduction

In the past several years, superconducting nanowire single-photon detectors (SNSPDs) in compact meander geometries have drawn extensive attention due to their high speed, picosecond jitter time, almost negligible dark count rate, and broad wavelength response especially for infrared single-photons.[1–4] This meander-style device is exploited to detect not only photons but also high energy particles such as bimolecular.[5] NbN is commonly used for SNSPDs, owing to its short electron–phonon coupling time (0.06 ns).[6] However, NbN-SNSPD with a large active area suffers large kinetic inductance of the very long nanowire, which leads to a long reset-time and, therefore, reduces the count rate. Nb could be an alternative material to solve this problem. Although the electron–phonon coupling time of Nb (0.37 ns)[6] is longer than that of NbN, the kinentic inductance of Nb is much smaller than that of NbN. This means that Nb SNSPD could have a high count rate.[7–9] Moreover, Nb-SNSPDs could be photon-number-resolved and spectrally sensitive due to a small resistance of the photon-induced normal state domains on Nb meander.[7] For these reasons, Nb is a promising alternative material for SNSPDs.

There have been previous studies on the superconducting properties and their relation to micro-structural detail.[10–14] However, there is seldom discussion about long Nb nanowires, due to the difficult fabrication process of very long nanowires up to several hundreds of micrometers. Meander-type structure provides an opportunity to study the transport properties of a long approximate quasi-one-dimensional nanowire. Furthermore, the SNSPD device performance could be modified by magnetic field. For example, the photon detection assisted by magnetic field has been discussed in Refs. [15] and [16]. The applied field increases the dark count rates, but also raises the photon detection efficiency. Therefore, understanding the properties of the Nb meander nanowires is of great importance for designing and improving the performance of the device.

In this paper, we focus on the superconducting properties of the meander nanowires. The critical temperature, critical field, and critical current are studied. For comparison, micro-bridge and thin film samples are also measured.

2. Sample fabrication

Nb films with thickness values from 4 nm to 100 nm were deposited onto 500-μm thick Si (100) substrate covered with an amorphous layer of 500-nm thick SiO_2. The deposition was carried out in a home-made ultra-high vacuum direct

*Project supported by the National Basic Research Program of China (973 Program) (Grant Nos. 2011CBA00106 and 2009CB929102) and the National Natural Science Foundation of China (Grant Nos. 11104333 and 10974243).

†Corresponding author. E-mail: dzheng@ iphy.ac.cn

© 2014 Chinese Physical Society and IOP Publishing Ltd

current (dc) magnetron sputtering system which has a background pressure lower than 10^{-9} mbar (1 bar = 10^5 Pa) owing to the very low leakage rate of the system and a built-in non-evaporable getter (NEG). The deposition was carried out from an Nb target of 99.95% purity at ambient temperature. The film thickness was determined by X-ray reflectivity (XRR), exclusive of the thickness of oxide layer (2 nm–3 nm) on the Nb films.

The thin films of about 7-nm thick were patterned into micro-bridges (25-μm wide, 100-μm long) connected with four electrodes and alignment marks by using photolithography and reactive ion etching (RIE) process based on Ar/SF_6 gas mixture. In a subsequent step, the meander lines were defined in the central area of Nb micro-bridges by means of e-beam lithography (EBL) and RIE. In the EBL process, the samples were spin-coated with PMMA 495 electron resist (positive tone) and the patterns were written at 20 kV by a Raith 150 EBL system with an area dose of 240 μC/cm^2. All the unwanted Nb films were removed by RIE down to SiO_2 afterwards. The detailed fabrication process of the specimens is illustrated in Fig. 1.

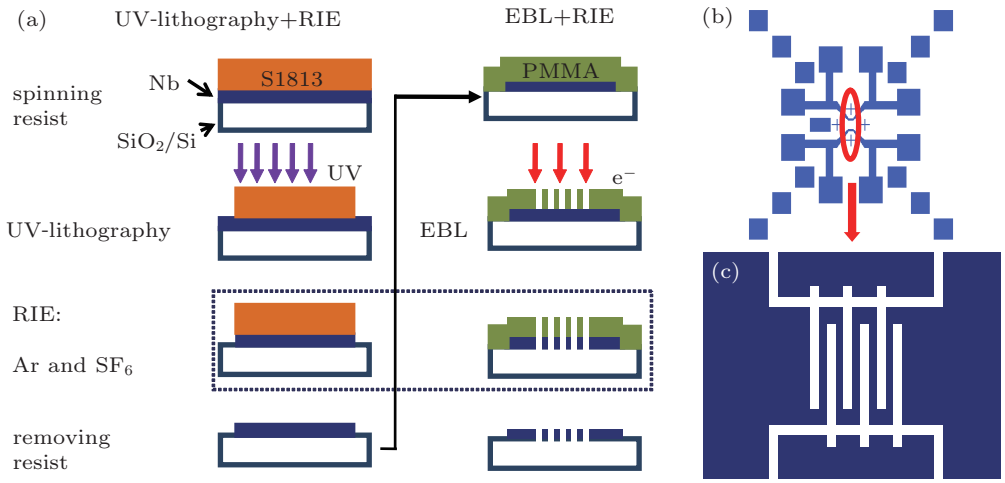


Fig. 1. (color online) (a) Schematic plot of the fabrication process of Nb meander nanowires. (b) A diagram of two micro-bridges and electrodes defined by UV-lithography and RIE. (c) A diagram of the meander nanowire on the central part of the micro-bridge. The white parts represent etched area.

Superconducting properties were determined from standard four-probe transport measurements carried out in a Quantum Design PPMS system with highest magnetic field up to 8 T and lowest temperature down to 1.8 K.

3. Results and discussion

For the meander samples, the width is around 100 nm and the total length is about 500 μm as shown by SEM image in Fig. 2. The enlarged image (Fig. 2(b)) shows very uniform meander structure with a filling factor of about 0.5. The profile of the meander wires is also examined by using atomic force microscope (AFM), which is shown in Fig. 3. The non-rectangular cross-sectional profile is believed to be due to the shape of the scanning probe. Because of the etching of SiO_2 layer on the substrate surface, the measured depth of trench is about 20 nm, more than twice the actual Nb film thickness.

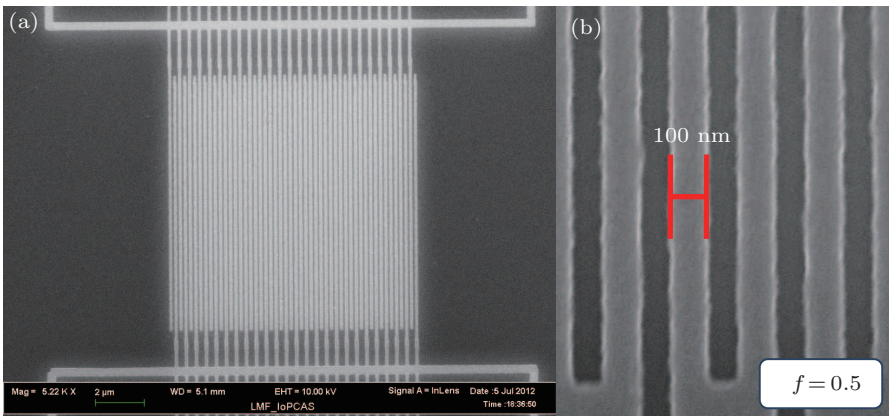


Fig. 2. (color online) (a) SEM image of an Nb meander nanowire sample with an active area of about 10 μm×10 μm. (b) The enlarged SEM image of panel (a). The width of the meander nanowire is around 100 nm and the filling factor is about 0.5.

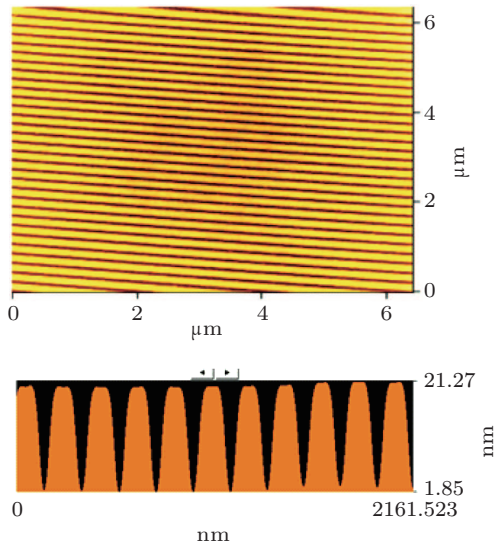


Fig. 3. (color online) AFM image of Nb meander nanowire over a 6 μm×6 μm area. The lower panel shows the height (≈ 20 nm) of the cross section profile. However, this value is not the actual thickness of Nb, because RIE based on Ar/SF_6 can also etch SiO_2.

In Fig. 4, we show the temperature dependences of resistance for a meander structure and a micro-bridge sample respectively. Clearly, the T_c is low and the transition broadens for the meander nanowire. The degradation of the long nanowire is mainly caused by the damages in the nano-fabrication process.

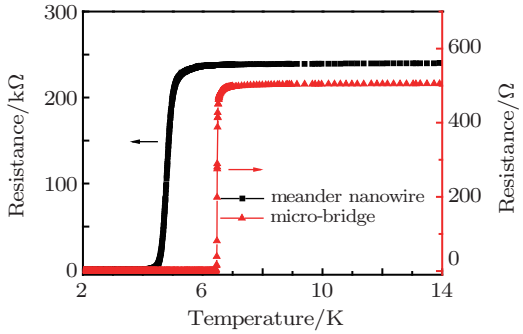


Fig. 4. (color online) Curves of resistance versus temperature (R–T) of the micro-bridge (red triangles) and meander nanowire (black squares). The solid lines are to guide the eye. The meander nanowire exhibits a T_c around 4.8 K, which is lower than that of micro-bridge due to the damages in the nano-fabrication process.

In Fig. 5, we show $R(T,H)$ curves measured in different magnetic fields for the samples, with the field applied in parallel and perpendicular to the sample surface respectively. The in-field measurements are performed a few weeks after measuring the zero-field R–T curve, and the oxidation of surface in the atmosphere reduces T_c of the specimen slightly. With increasing magnetic field, the transition is shifted toward lower temperatures but exhibits almost no broadening. We define the mid-point of the transition as the critical temperature, and the superconducting phase diagrams (H–T_c/T) are obtained and shown in Fig. 6. Notably, the parallel critical field $H_{c\parallel}$ is much larger than the perpendicular critical field $H_{c\perp}$. It is known that the Gibbs free energy of a superconductor is increased with increasing magnetic field, and the critical field is obtained when the Gibbs free energy is increased to a value equal to the superconducting condensation energy. For ultra-thin film samples, the parallel field can penetrate into the total thickness. This reduces the increasing values of the Gibbs free-energy compared with the bulk samples. Therefore for the ultra-thin specimens, $H_{c\parallel}$ is larger than $H_{c\perp}$.

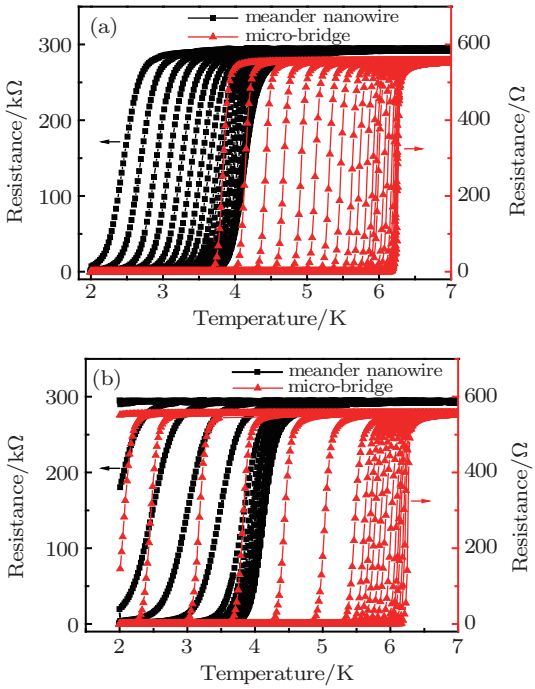


Fig. 5. (color online) Curves of resistance versus temperature (R–T), measured in a series of magnetic fields. (a) Parallel fields from 0 T up to 8 T (0, 0.02, 0.04, 0.06, 0.08, 0.1, 0.15, 0.2, 0.25, 0.3, 0.35, 0.4, 0.5, 0.8, 1.2, 1.6, 2, 2.4, 2.6, 2.8, 3.2, 3.6, 4, 4.5, 5, 5.5, 6, 6.5, 7, 7.5, and 8, from right to left) are applied for both meander nanowire (black squares) and micro-bridge (red triangles). (b) Perpendicular fields from 0 T up to 1.6 T (0, 0.02, 0.04, 0.06, 0.08, 0.1, 0.15, 0.2, 0.25, 0.3, 0.35, 0.4, 0.5, 0.8, 1.2, and 1.6, from right to left) are applied for these two specimens. With raising field, all R–T curves move toward lower temperatures, but all the transitions are not apparently broadened.

We find that the $H_{c\parallel}$–t ($t = T_c/T$) data of both the meander nanowire and the micro-bridge samples show clearly bending curvature in the temperature range just below T_c. This is typical for very thin superconducting films with the film thickness much smaller than the penetration depth. The data could be fitted to the following relation[10]

$$H_{c\parallel}(t) = H_{c\parallel}(0)\left\{\left(1-t^2\right)/\left(1+t^2\right)\right\}^{1/2}. \quad (1)$$

This relation is based on the Ginzburg and Landau (GL) theory using the temperature dependence of the two-fluid model. For ultra-thin film with thickness d (d is smaller than the coherence length), the parallel critical field is about $2\sqrt{6}\lambda H_c/d$,[17] where λ and H_c are the penetration depth and the thermodynamic critical field of bulk material. In the two-fluid model,

the temperature dependence of λ follows $(1-t^4)^{-1/2}$ while H_c follows $(1-t^2)$, leading to Eq. (1). The two $H_{\|}$–t curves are almost the same, which demonstrates that the meander structure on the central part of micro-bridge has negligible influence on $H_{c\|}$.

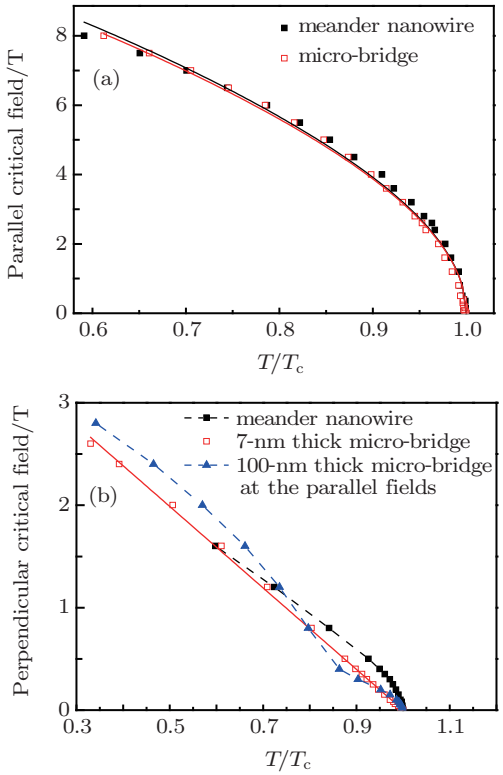


Fig. 6. (color online) Dependences of the critical field on T/T_c of the nanowire (black squares) and micro-bridge (red empty squares). (a) At parallel field, the solid lines are the fitted results by Eq. (1). (b) At perpendicular field, the dashed line is guideline only, and the red line is the fitting result to the linear temperature dependence which is proportional to $1-t$. The blue triangles are the data of the $H_{c\|}$–t curve of a 100-nm thick Nb micro-bridge.

However, a notable difference exists between the $H_{\perp}$–t curves of the micro-bridge and the meander nanowire. For the micro-bridge sample, the perpendicular critical field $H_{c\perp}$ shows linear temperature dependence as would expect from the GL theory.

According to GL equation,

$$H_{c\perp}(t) = \varphi_0/2\pi\xi^2(t), \quad \xi(t) = \xi(0)(1-t)^{-1/2}, \qquad (2)$$

where ϕ_0 is the flux quantum, and ξ is the coherence length. From a linear fitting, the extrapolated values of $H_{c\perp}(0)$ of both specimens are obtained. According to Eq. (2), the values of $\xi(0)$ is obtained to be 6.5 nm for the micro-bridge.

For the nanowire sample, we see that $H_{c\perp}$ is almost linear at lower temperatures, but shows a bending curvature in the vicinity of T_c ($> 0.95T_c$) like the case of parallel field. The obvious curvature in $H_{c\perp}$ near T_c has also been studied in thin Nb films (5-nm–10-nm thick) which was explained by using localization effect,[18] but has not been seen in meander nanowires. Obviously, in our experiments, this curvature is due to the patterned meander-type structure, instead of thin thickness.

We believe that the nonlinear behavior of $H_{\perp}$–t is caused by two reasons. On the one hand, although the width of the nanowire ($\sim$ 100 nm) is much larger than the thickness, it is still comparable to the coherence length of Nb near T_c (which is about 26 nm at $t \sim 0.95$). Furthermore, the coherence length increases with increasing temperature and diverges at T_c. Thus, at temperatures close to T_c, the superconducting order parameter could be regarded as constant as in the case of ultra-thin films. Thus, in the temperature range close to T_c, it is not surprise to observe a bending behavior. As temperature decreases, the coherence length is reduced. Then $H_{\perp}$ shows linear temperature dependence. This kind of crossover could not be seen in bulk samples because the crossover temperature is very close to T_c. For nanowire samples, the dimension is small and it can be seen more clearly. In order to further confirm this explanation, the $H_{\|}$–t curve of a 100-nm thick Nb micro-bridge sample is measured in parallel field. Near T_c, a notable curvature is shown, and as the field increases until t reaches 0.87, $H_{\|}$–t curve is an approximate linear dependence. The $H_{\|}$–t behavior ($0.87 < t < 1$) of 100-nm thick micro-bridge is similar to the $H_{\perp}$–t dependence of the meander. Therefore, for the meander wire, the nonlinear curve near T_c is probably caused by the limitation of the width of nanowire. In addition, the relationship between d and $\xi(t)$ determines the $H_{\|}$–t behavior.[10] For 100-nm thick Nb micro-bridge, $t = 0.87$ is a turning point, where $d \sim \xi(t)$. As t decreases, the curve is approximately linear.

On the other hand, the stronger localization effect for the meander line than that of the micro-bridge may lead to bending curvature as we observed in Ref. [18]. However, since $H_{\perp}$–T curve is linear for thin film and microbridge samples, it is possible that the localization does not play a major role here. Nb on SiO_2/Si is polycrystalline which can be confirmed by SEM images and XRD results. For the ultra-thin Nb film, the sizes of grains are very small, thus the film is highly disordered. Moreover, when the meander nanowire sample is made, there could be additional defects introduced in the fabrication process along the edges of the nanowire. For these disordered sufficiently long quasi-one-dimensional nanowire structures,[19] the normal resistance of the nanowire before transition $R_N(\approx 165\ \mathrm{k}\Omega)$ is very large, and the resistivity of the nanowire (34 $\mu\Omega$·cm) is larger than that of the micro-bridge (23 $\mu\Omega$·cm). It probably leads to a stronger localization effect of the electrons than that of the micro-bridge specimen.[20] The nonlinear behavior of $H_{\perp}$–T curve near T_c may be partially attributed to the stronger localization effect as indicated in Ref. [18].

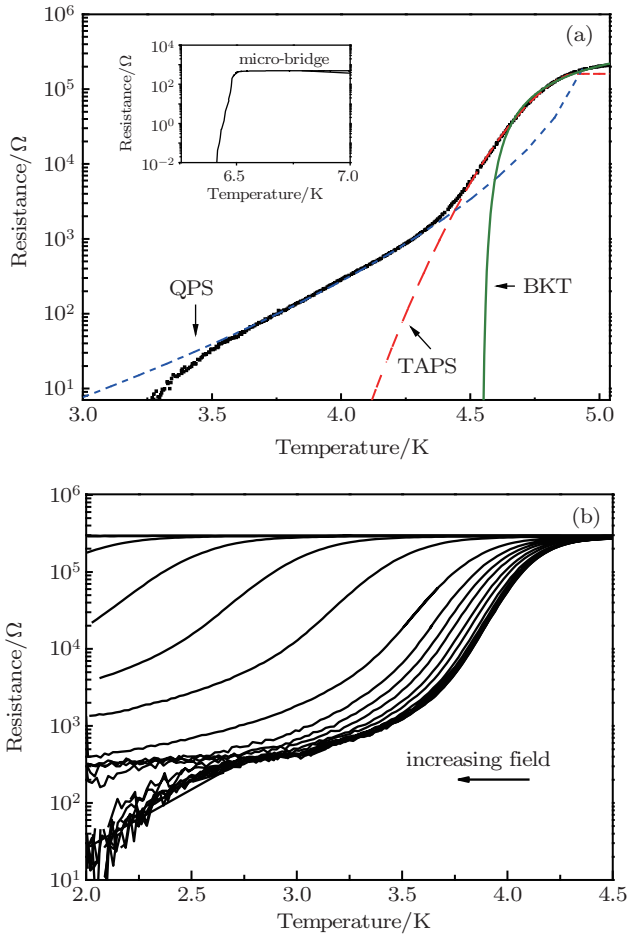


Fig. 7. (color online) $R(T)$ data for the meander nanowire. (a) At zero-field, the transition is measured. At around T_c, the transition is fitted by using Eq. (3) (red dash line), while at lower temperature, the transition tail exists, which can be fitted by QPS theory (blue short dash line). BKT model is used to fit the transition (green thin solid line). The inset shows the $R(T)$ curve of the micro-bridge. (b) $R(T)$ measurements for the meander nanowire in the fields from zero up to 1.6 T (from right to left).

The R–T curves of meander and micro-bridge are further analyzed as shown in Fig. 7(a). The R–T curve of meander has a tail at low temperature, while there is no tail behavior for the micro-bridge. The micro-bridge can be seen as two-dimensional structure because the width of the structure is much larger than ξ and λ. Therefore we believe that the R–T tail for the meander nanowire is due to the limitation of the dimension. From the behavior of the R–T curve of the nanowire, the transition is almost the same as those of the quasi-one-dimensional structures studied in Refs. [13], [16], [21], and [22]. The transition can be described by thermally activated phase slips (TAPS), which is strongly pronounced near T_c.[21,22] Little's phase slip theory is the simplest approximation of describing TAPS.[21,23] According to Little's equation[21]

$$R(T) = R_N \exp\left(-\frac{\Delta F}{kT}\right), \tag{3}$$

where $\Delta F \approx 0.83\,[L/\xi(0)]\,(R_Q/R_N)\,kT_c\,(1-T/T_c)^{3/2}$ is the free-energy barrier, $R_Q = h/4e^2 = 6.45\ \mathrm{k\Omega}$ is the quantum resistance for Cooper pairs, and k is the Boltzmann constant. Our data are fitted well to Eq. (3) near T_c. The Berezinsky–Kosterlitz–Thouless (BKT) transition model in two-dimensional systems is also used to fit the results near T_c using formula (3.7) in Ref. [24]. However, the data deviate from the fitting line. Therefore, we suggest that the quasi-one-dimensional model is more suitable for the meander specimen.[24]

However, the resistance tail at lower temperature deviates from Little's theory notably. Usually the quantum phase slip (QPS) theory is used to explain the resistance tail of the transition.[13,22] Our result is nearly fitted to QPS theory through using formula (2) in Ref. [22], except in the temperature range below 3.5 K. As the applying magnetic field increases, the probabilities of TAPS and QPS increase, which induces the raising of the resistance at the temperature less than T_c. As the applying magnetic fields increases, the probability of phase slip increases. This could lead to increased dark count when the meander nanowire is used as a single photon detector. Indeed, it has been reported that the dark count rate and the detection efficiency of SNSPDs are both proportional to the number of potential phase slip centers.[16]

Current–voltage curves of the meander are measured in the current-biased conditions and at various temperatures below T_c. The I–V characteristics show sharp jumps at $I_c(T)$ and hysteresis behaviors with the return current I_r as illustrated in Fig. 8(a). At 2 K, a strong hysteresis behavior is observed. The critical current density (j_c) evaluated from I–V characteristics is about 2.8×10^6 A/cm^2 at 2 K, which is more than ten times smaller than that of the micro-bridge (3.6×10^7 A/cm^2 at 2 K). The decreasing of j_c is another evidence for the damage of the edge areas of the nanowire. As temperature increases approximately to T_c, both I_c and I_r decrease, however, the hysteresis behaviors become smaller. For a long nanowire, the I–V hysteresis has been illustrated using a simple model of a localized normal hotspot maintained by Joule heating.[25,26] When the current is lower than I_c, the specimen keeps superconducting state without dissipation. When the biased current increases to I_c, an unstable hotspot is formed and the nanowire transition takes place quickly from zero resistance state to normal state. With scanning current decreasing, the hotspot maintains the normal state until the current reaches I_r due to Joule heating, where I_r is the minimum current to sustain a normal hotspot. This model predicts that I_r is proportional to $(1-t)^{1/2}$[25]

$$I_r \cong I_r(0)\,(1-t)^{1/2}. \tag{4}$$

The I_r–t curve of the meander nanowire is plotted in Fig. 8(b), which is well fitted to Eq. (4). The dependence of I_c on t , which we obtained, generally follows the mean-field behavior predicted by the GL theory:[25]

$$I_c = I_c(0)\,(1-t^2)^{3/2}(1+t^2)^{1/2}, \tag{5}$$

where the fitting coefficient $I_c(0)$ is 87.4 μA. I_c and I_r have different dependences of temperature as can be seen in Fig. 8(b), therefore the hysteresis behaviors become weaker when increasing the temperature.

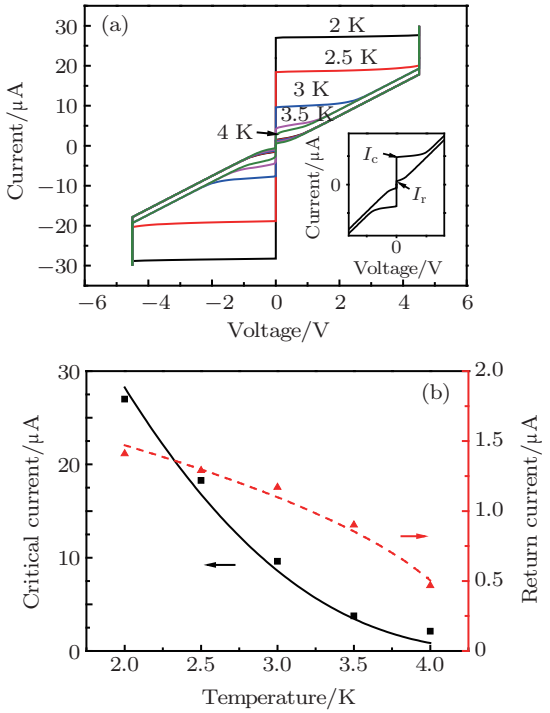


Fig. 8. (color online) Measurements of critical current for the nanowire. (a) Current–voltage characteristics of the meander wire at temperatures from 2 K to 4 K. When the current biased through the nanowire is larger than I_c, the whole nanowire becomes normal state following Ohm's law. The voltage is restricted to around 4 V due to the measuring range restriction of the voltmeter. The inset defines I_c and I_r. (b) I_c (black squares) and I_r (red triangles) dependences of temperature for the nanowire. I_c–T curve are fitted by Eq. (4) (black solid line). The red dash line is the fitting result of I_r–T using Eq. (5).

4. Conclusions

We here present the fabrication of the meander structures based on ultra-thin Nb films for SNSPDs by EBL process. Also, superconducting properties of meander strips are studied systematically. $H_{c\parallel}(t)$ and $H_{c\perp}(t)$ curves of both the meander specimen and micro-bridge are obtained from a series of $R(T,H)$ at different applied magnetic fields up to 8 T, which are parallel or perpendicular to the specimens. The results illustrate that nanostructures on the Nb films have almost no effect on $H_{c\parallel}$. However, the $H_{c\perp}(t)$ curve of meander line behaves in a different manner from that of micro-bridge when T approaches to T_c, showing a down turn curvature. In other words, the $T_c(H)$ value of meander line change little with increasing the magnetic fields when the field is weak, while $H_{c\perp}$ presents a linear dependence of t at high fields but is not fitted to GL equation. The nonlinear behavior of $H_{c\perp}$ in the nanowire is attributed to the fact that the coherence length becomes larger than the line width in the vicinity of T_c. Additionally, the localization of carriers in the nanowire could also partially contribute to the nonlinear behavior. The resistive transitions could be described by the phase-slip model for quasi-one-dimensional system. Moreover, $I_c(t)$ and $I_r(t)$ of meander nanowire can be illustrated using a simple model of a localized normal hotspot maintained by Joule heating. Studying the properties of the meander structures based on ultra-thin Nb films in varying fields will be beneficial for designing and improving the performances of SNSPDs with the assistance of field.

Acknowledgment

The authors thank Yang H F for helpful discussions about EBL technique, Zhang Y Z for technical assistance with PPMS.

References

[1] Hadfield R H 2009 *Nat. Photonics* **3** 696
[2] Gol'tsman G N, Okunev O, Chulkova G, Lipatov A, Semenov A, Smirnov K, Voronov B, Dzardanov A, Williams C and Sobolewski R 2001 *Appl. Phys. Lett.* **79** 705
[3] Marsili F, Verma V B, Stern J A, Harrington S, Lita A E, Gerrits T, Vayshenker I, Baek B, Shaw M D, Mirin R P and Nam S W 2013 *Nat. Photonics* **7** 210
[4] Zhang C and Jiao R Z 2012 *Chin. Phys. B* **21** 120306
[5] Zen N, Suzuki K, Shiki S and Ohkubo M 2009 *Physica C* **469** 1684
[6] Parlato L, Latempa R, Peluso G, Pepe G P, Cristiano R and Sobolewski R 2005 *Supercond. Sci. Technol.* **18** 1244
[7] Annunziata A J, Frydman A, Reese M O, Frunzio L, Rooks M and Prober D E 2006 *Advanced Photon Counting Techniques* **6372** 63720V
[8] Fujii G, Fukuda D, Numata T, Yoshizawa A, Tsuchida H, Inoue S and Zama T 2009 *QuantumCom LNICST* **36** 220
[9] Annunziata A J, Santavicca D F, Chudow J D, Frunzio L, Rooks M J, Frydman A and Prober D E 2009 *IEEE T Appl. Supercond.* **19** 327
[10] Asada Y J and Nosé H 1969 *J. Phys. Soc. Jpn.* **26** 347
[11] Delacour C, Ortega L, Faucher M, Crozes T, Fournier T, Pannetier B and Bouchiat V 2011 *Phys. Rev. B* **83** 144504
[12] Kim Y W, Kahng Y H, Choi J H and Lee S G 2009 *IEEE T Appl. Supercond.* **19** 2649
[13] Rogachev A and Bezryadin A 2003 *Appl. Phys. Lett.* **83** 512
[14] Tettamanzi G C, Pakes C I, Potenza A, Rubanov S, Marrows C H and Prawer S 2009 *Nanotechnology* **20** 465302
[15] Bulaevskii L N, Graf M J and Kogan V G 2012 *Phys. Rev. B* **85** 014505
[16] Herder C H 2009 "Study of Ultranarrow Superconducting NbN Nanowires and Nanowires under Strong Magnetic Field for Photon Detection" (BS Dissertation) (Cambridge: Massachusetts Institute of Technology)
[17] Tinkham M 1996 *Introduction to Superconductivity*, 2nd edn. (Singapore: McGraw-Hill) pp. 141–143
[18] Quateman J H 1986 *Phys. Rev. B* **34** 1948
[19] Annunziata A J 2010 "Single-Photon Detection, Kinetic Inductance and Non-equilibrium Dynamics in Niobium and Niobium Nitride Superconducting Nanowires" (Ph. D. Dissertation) (New Haven: Yale University)
[20] Costa A T Jr , Muniz R B, Jisang Hong and Wu R Q 2004 *Europhys. Lett.* **67** 254
[21] Bezryadin A 2008 *J. Phys.: Condens. Matter* **20** 043202
[22] Lau C N, Markovic N, Bockrath M, Bezryadin A and Tinkham M 2001 *Phys. Rev. Lett.* **19** 217003
[23] Little W A 1967 *Phys. Rev.* **156** 396
[24] Kitaygorsky J 2008 "Photon and Dark Counts in NbN Superconducting Single-Photon Detectors and Nanostripes" (Ph. D. Dissertation) (Rochester: University of Rochester)
[25] Skocpol W J, Beasley M R and Tinkham M 1974 *J. Appl. Phys.* **45** 4054
[26] Stockhausen A, Il'in K, Siegel M, Södervall U and Jedrasik P 2012 *Supercond. Sci. Technol.* **25** 035012